SSC20-WKVIII-05

Pointing Enhancement for an Optical Laser Downlink Using Automated Image Processing

Sebastian Wenzel, Steffen Gaisser, Christian Kley, Johannes Reinhart, Sabine Klinkner
University of Stuttgart Institute of Space Systems
Pfaffenwaldring 29, 70569 Stuttgart, Germany
sebastian.wenzel@irs.uni-stuttgart.de

ABSTRACT

The small satellite *Flying Laptop*, launched in July 2017, was developed and built by graduate and undergraduate students at the Institute of Space Systems of the University of Stuttgart with support by space industry and research institutions. The mission goals are technology demonstration, earth observation, and serving as an educational satellite. At a mass of 110 kg, it features three-axis stabilized attitude control and several payloads, including an AIS receiver, a multi spectral camera system, a wide angle camera, and an optical communication terminal.

The pointing requirement for the optical communication is an accuracy of less than 150 arcseconds during a target overflight. To fulfill this requirement, several measures are needed. A major part of them is the characterization of the attitude control system (ACS). Since there is no optical receiver onboard, it is not possible to perform closed loop tracking of the satellite attitude. Therefore, the absolute performance and the characteristic noise levels of the attitude control system, can only be determined with other payloads. In this case the multi-spectral camera system was used, providing a ground resolution of 25 m. To use the images from the satellite to improve the ACS, three steps have to be taken. As a first action, the images have to be georeferenced to know the position of each pixel in the WGS84 coordinate system. With this information, the deviation of the image center from the desired target is measured. This second step includes the calculation of the deviation matrix. To avoid a corruption of the attitude control of the satellite, the matrix is checked for unrealistic values in a third and final step. These three actions can be repeated as needed without human interaction.

By updating the ACS model onboard the satellite, the results of the image processing are used to correct the off-pointing. This deviation is time invariant and is caused by an insufficient alignment of the satellite axes and the cameras on ground. In contrast to that, characterizing noise as a time variant factor, the ACS is tested over a long period of time. This is achieved by analyzing images from one, as well as from multiple target overflights. This conquers the issue of a very low image rate while observing high frequency attitude changes. Using this mechanism, the proposed process can be used to continuously monitor the pointing quality.

As a first approach the described processing is done manually by comparing the target position on Earth with the center of the taken image. The method successfully showed an improvement of the pointing in the pictures, paving the way for their automation. This paper gives an overview of the needed image processing and tools to automatically use cameras on board the satellite to validate and improve the ACS periodically. First results of the long term characteristics and pointing improvements are shown.

INTRODUCTION

The small satellite *Flying Laptop* carries an optical communication system OSIRISv1 from the German Aerospace Center (DLR) as a payload.[1] This payload offers a high speed communication for payload data from orbit to an optical ground station. However, the beam divergence of the laser is only $1.2\,\mathrm{mrad}$ and the satellite receives no feedback from the ground. Therefore, the pointing accuracy must be verified and improved in a different way. Additionally, the knowledge of the dynamics of the pointing to the ground station might be improved. This is the reason why target pointings with the Multispectral Imaging Camera System (MICS) of *Flying Laptop* were used instead of inertial pointings.
The described methods are an approach to improve the pointing using MICS images with the measured satellite attitude, position and time. The main outcome of the described methods is therefore not the georeferenced image, but the more accurate satellite attitude. Nevertheless, the implemented single image georeferencing can be used for future satellite applications.

The Flying Laptop Satellite

The small satellite *Flying Laptop* launched in July 2017, was developed and built by graduate and undergraduate students at the Institute of Space Systems of the University of Stuttgart with support by space industry and research institutions. The spacecraft is three-axis-stabilized and uses Star Cameras and Fiber-optic-gyros to determine its current attitude. At a mass of $110\,\mathrm{kg}$ it has a size of $60\,\mathrm{cm} \times 70\,\mathrm{cm} \times 87\,\mathrm{cm}$. The desired absolute performance error is $150''$ during a target pointing towards the ground station. *Flying Laptop* uses two cold-redundant Cobham Gaisler UT699 as onboard computers, which communicate through two IO Boards from 4Links with all bus equipment. Additionally, the satel-

lite has an FPGA payload onboard computer (PLOC) to communicate with its payloads. Besides the MICS and OSIRISv1, those payloads include a panorama camera (PAMCAM), an AIS receiver and a 10 Mbit/s S-Band Data Downlink System. The PLOC is commanded by the Onboard Computer (OBC) via the IO Boards.

The Multispectral Camera System

As the the *Flying Laptop* Satellite is designed to observe vegetation on earth, it utilizes a camera system with the three channels green, red and near infrared. The MICS is the main payload of the satellite with a ground resolution of roughly $25\,\mathrm{m}$ and a $1024\,\mathrm{px} \times 1024\,\mathrm{px}$ interline CCD sensor. This results in a swath width of roughly $25.6\,\mathrm{km}$ at a height of $600\,\mathrm{km}$. The camera system is controlled by the PLOC. This includes the trigger mechanism of a picture. Although, the PLOC is commanded to take a picture by the OBC, the PLOC writes its internal time stamp in the meta data of the picture. In contrast to that, the current attitude and position is recorded by the OBC and sent to the PLOC in the *Take Picture* command.

Approach

In the course of this paper an image of the coast of Dubai is used to illustrate the process. The original image used as example can be seen in figure 1. It was taken by the near infrared channel of the MICS on the 29th of May 2019, 6:25 UTC.

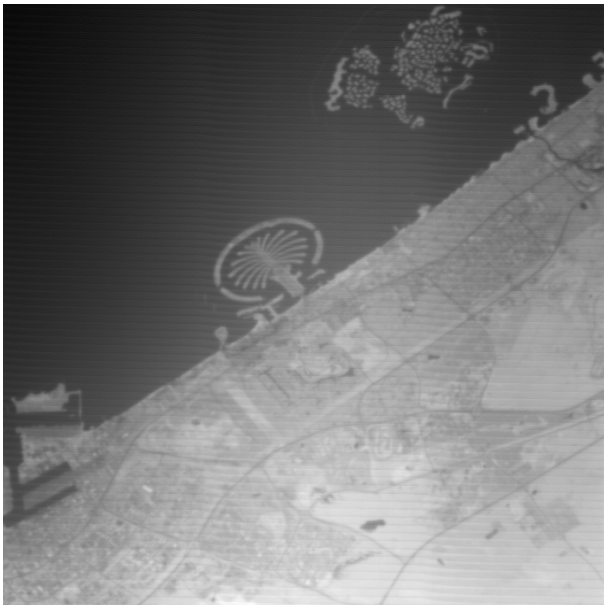

Figure 1: Original image as sent from the satellite

The approach described in this paper can be divided into five parts. The first step is the orthorectification of the camera images. The second step is the alignment of the orthorectified images with sentinel images. This is later referred to as georeferencing. Using this image and its geodata, a resection can be performed to determine the actual external camera parameters in a third step. Within the fourth step, the external camera parameters are used to determine the attitude deviation of the satellite. With this information, a more precise camera installation matrix can be created and uploaded to the satellite as a fifth and final step. The work flow for the image preparation and processing part can be seen in figure 2.

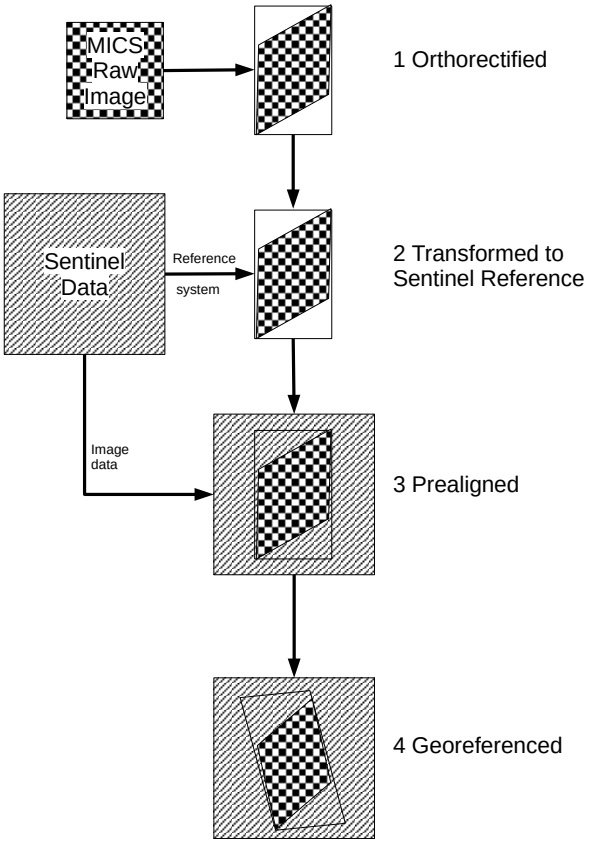

Figure 2: Image Processing Flow

ORTHORECTIFICATION

An orthophoto is an aerial image that is corrected for geometric distortions coming from camera tilt angles, the topographic relief and lens distortions. For the MICS images taken by the *Flying Laptop* satellite in target pointing mode, the camera tilt angle is the dominant error. In the course of this paper we use the expression *orthophoto* to describe an aerial image mainly corrected from this camera tilt angle. Removing image distortions using the preliminary on-board attitude information yields a starting point for further image processing.
Two coordinate systems are relevant for the transformation between the camera pixels and the world coordinates. The first one is the Earth Centered, Inertial system (ECI). This is the reference system of the *Flying Laptop* attitude. The second one is the Earth centered, Earth Fixed system (ECEF) in which the position of *Fly-*

ing Laptop is defined and most of the described calculations are done.
The goal of the orthorectification is to find a corresponding world coordinate for every image coordinate by only using image meta data from the camera as well as the satellite. This can be achieved by using the pinhole camera model to transform world coordinate points into pixel coordinates as displayed in equation (1). The description of the pinhole camera model and therefore the orthorectification process is based on *Multiple View Geometry in Computer Vision* from Hartley et al.[2]

$$\begin{bmatrix} s \cdot x_b \\ s \cdot y_b \\ s \end{bmatrix} = P \cdot \begin{bmatrix} X \\ Y \\ Z \end{bmatrix} \tag{1}$$

The vector $[x_b \ y_b]^T$ represents pixel coordinates and $[X \ Y \ Z]^T$ are the corresponding world coordinates. The projection matrix P can be described as:

$$P = K[R| - C] \tag{2}$$

where K consists of the intrinsic camera parameters:

$$K = \begin{bmatrix} f_{px} & 0 & x_p \\ 0 & f_{px} & y_p \\ 0 & 0 & 1 \end{bmatrix} \tag{3}$$

with f_{pix} being the focal length in pixel, x_p and y_p describing the optical center of the camera.
The second part of P consists of the extrinsic camera parameters, where R describes the rotation between the camera system and the Earth Centered, Earth Fixed system:

$$R = R_{MountingBias} \cdot R_{Attitude} \cdot R_{ecef2eci}(t_{Photo}) \tag{4}$$

In this equation, $R_{MountingBias}$ is the deviation of the MICS to the *Flying Laptop* system. $R_{Attitude}$ describes the satellite's attitude from ECI to the *Flying Laptop* system and $R_{ecef2eci}$ being the transformation matrix between the ECEF and ECI System at the time of the photo t_{Photo}.
In addition, C contains the translational part which depends on the satellite position:

$$C = R^T \cdot \begin{bmatrix} X_{Sat} \\ Y_{Sat} \\ Z_{Sat} \end{bmatrix}_{ECEF} \tag{5}$$

With the intrinsic and extrinsic camera parameters, an estimation of the observed area can be made by intersecting the camera field of view with an ellipsoid model, in our case WGS84, of the earth. This area defines the regular grid in world coordinates for the orthorectified image. Using these coordinates and formula (1), each grid element can be transformed into pixel coordinates. By interpolating the image gray values at these pixel coordinates onto the regular grid, the orthophoto, shown in figure 3, is created. It corresponds to step 1 in figure 2. The height model for the images is taken from ALOS data, freely available online.

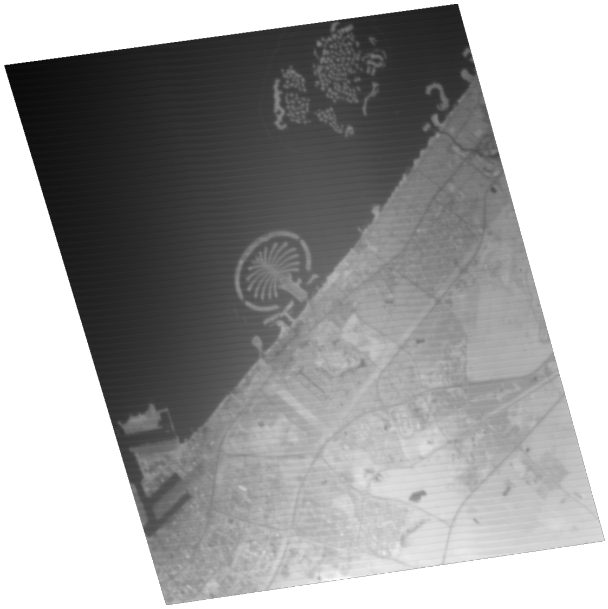

Figure 3: Orthorectified image

GEORECTIFICATION USING SENTINEL DATA

Orthorectifying the images mapped them to a surface model of the earth as described in the previous section. The result only uses the satellite's attitude and position and is therefore highly dependent on their precision. To determine the occurring deviations in the satellite position and attitude, one has to know which scene the image actually displays. The precise location of every pixel in world coordinates is retrieved by aligning the raw MICS image with external image data. This process can be seen as creating control points with known world coordinates for each pixel.

In our case sentinel data was used, to compare the MICS images to, since it is available to the public. With the Copernicus hub, an API is provided to automize the download of these data sets. The images to download were selected to match the world coordinates of the raw image as well as the camera channel. From the available sentinel images, the one with the least cloud coverage and latest time stamps was used. After retrieving the data from the copernicus hub, two steps, described in the following, are necessary to align the MICS images and the reference images from sentinel: prealigning the images and iteratively matching them.

Prealignment

As an initial guess for the image alignment of the MICS images with the sentinel data, the world coordinates retrieved from the orthorectification are used. This is referred to as prealigning the images. However, the ground resolution of the used sentinel data is with $10\,\mathrm{m}$ roughly 2.5 times higher than the MICS images. Therefore the resolution of the sentinel images is lowered before they can be used for the prealignment. For the tested data, the coordinate system of the MICS orthophotos was adapted from EPSG:4326 to EPSG:32640 to match the reference system as another preparation step. This transformation also includes changing the image data, since the two coordinate frames might not utilize the same axes. The image is now in the condition illustrated in step 2 of figure 2.
With now having the same ground resolution and reference frame the images are prepared to be prealigned by simply matching their world coordinates. The result after prealigning the images is shown in figure 4. It contains the sentinel image overlayed by the orthorectified MICS image. The deviation between the two images shows the offset between the satellite's pointing knowledge and the actual world coordinates.

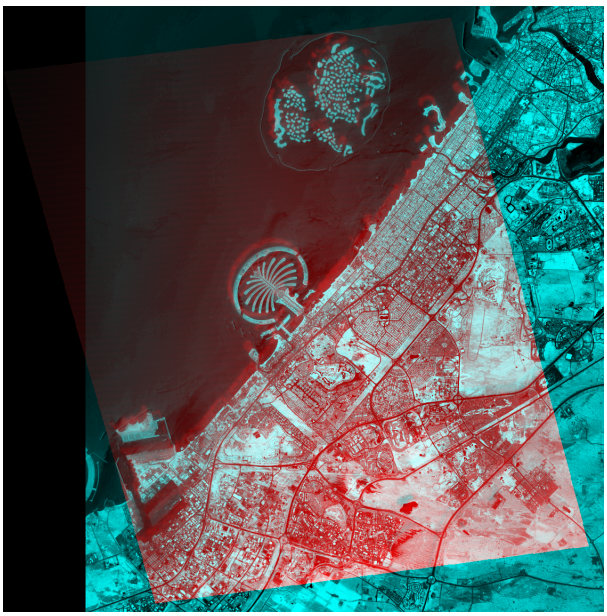

Figure 4: Sentinel image (cyan) overlayed with prealigned orthorectified MICS image (red)

Iterative Image Alignment

To further align the images, it is necessary to use image processing. An image alignment algorithm based on the *Enhanced Correlation Coefficient*[3] was used. This alignment technique is invariant to photometric distortions in contrast and brightness and is therefore well suited for images taken with different instruments. Nevertheless, as a measure to account for the different image properties, aligning is done in the gradient domain.
To align the images, the matrix A is determined, shifting the original pixel coordinates $[x\ y]^T$ according to formula (6) to the new coordinates $[x'\ y']$.

$$\begin{bmatrix} x' \\ y' \end{bmatrix} = A \cdot \begin{bmatrix} x \\ y \\ 1 \end{bmatrix} = \begin{bmatrix} a_1 & a_2 & t_1 \\ a_3 & a_4 & t_2 \end{bmatrix} \cdot \begin{bmatrix} x \\ y \\ 1 \end{bmatrix} \tag{6}$$

The matrix $\begin{bmatrix} a_1 & a_2 \\ a_3 & a_4 \end{bmatrix}$ represents the affine part of the transformation whereas $[t_1\ t_2]^T$ represents the translational part.
Since there can still be a significant offset between the images after the prealignment, it was chosen to use an iterative approach where different scale levels of the input images are used. By down-scaling the images, the stability of the alignment can be improved. The improvement is a consequence of the offset spreading over fewer, larger pixel. An example with two scale factors is shown in figure 5.

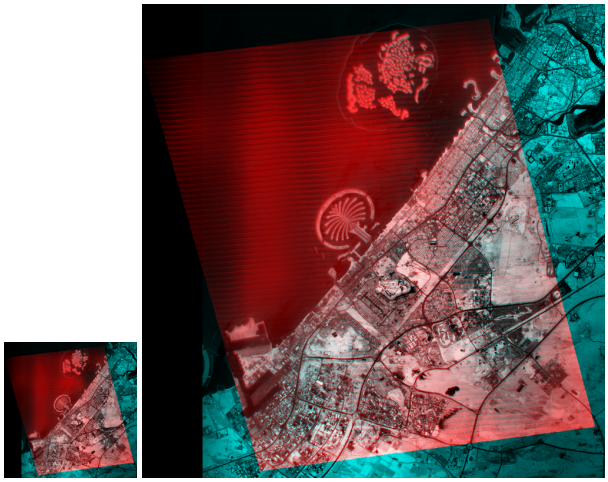

Figure 5: Alignment steps with scale factors 0.2 (left) and 0.7 (right)

The major influence to the image offset shown in figure 4 is described by translational motion. This can be verified by looking at the result of the alignment in equation (7). The complete image alignment flow is shown in figure 6. It can be seen that the scaled images were only used to reduce the translational offset of the images. This approach significantly reduces the processing time and stability of the proposed procedure. In figure 5 it can be seen that after the first iteration with a scale factor of 0.2, a big portion of the translational deviation is already compensated. The image is translated by $[t_1\ t_2]^T = [-9.196\ \ -15.199]^T$ pixels in the first iteration and by another $[t_1\ t_2]^T = [0.155\ 0.18]^T$ pixels after the second one, both coordinates measured in original scale. After applying the translational correction to

the full scale MICS image, the affine transformation was determined.

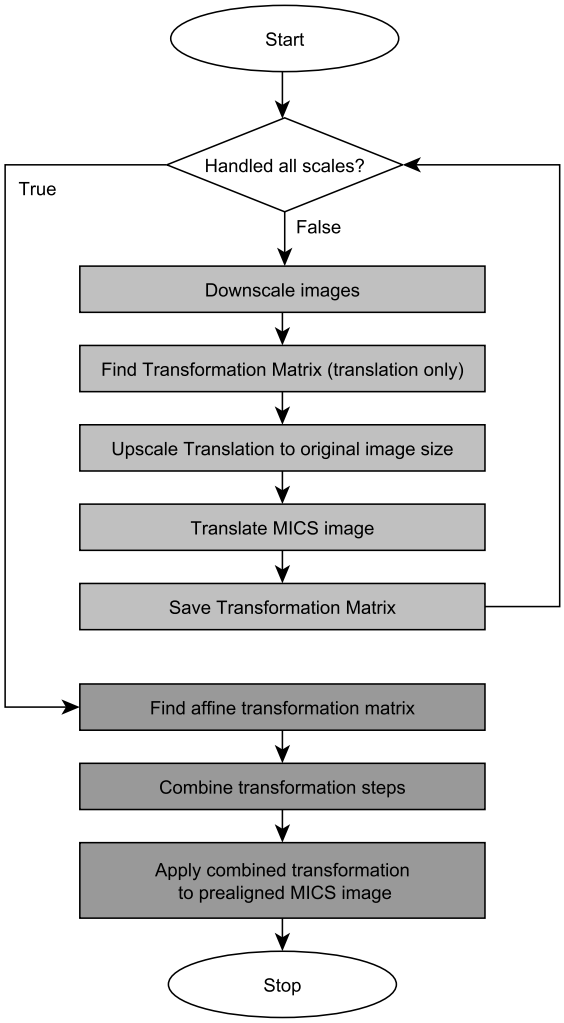

Figure 6: Iterative Alignment

Along with aligning the two images, the pixel transformations between the steps are tracked and finally combined to a transformation matrix.

The combined affine transformation for the presented image results in the matrix A, measured in pixel:

$$A = \begin{bmatrix} 1.0043 & 0.0045 & -17.3911 \\ -0.0039 & 1.0084 & -20.1604 \end{bmatrix} \tag{7}$$

The result of the alignment is a georeferenced MICS image as shown in figure 7. It is representing the result of step 4 in figure 2. With the georeferenced MICS image and by backtracking and combining all transformation steps in figure 2 it is now possible to bind a world coordinate to each raw image pixel coordinate.

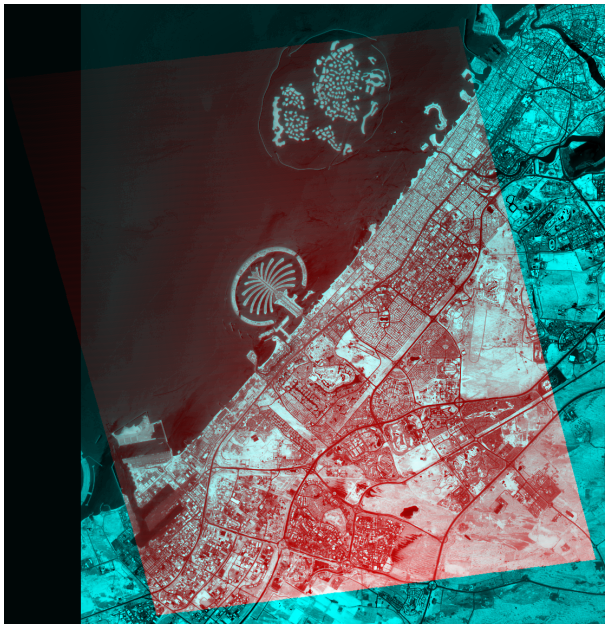

Figure 7: Sentinel (blue) image overlayed with aligned MICS image (red)

RESECTION

To this point of the process, all data was used to map the images on the surface of the earth as precise as possible. By using the georeferenced image it is now feasible to calculate the actual satellite attitude for the time the image was taken.

A resection is solving the transformation between camera sensor coordinates and world coordinates and is depending on the external camera parameter. The implemented resection used for this paper, was mainly adapted from the book *Introduction to Modern Photogrammetry* by Edward M. Mikhail et al.[4] For the Resection process, the relation in equation (1) can be used in an adapted form to solve the transformation between the georeferenced world coordinates and the MICS raw pixel coordinates. This results in the transformation displayed in the following equation:

$$\begin{bmatrix} x \\ y \\ -f \end{bmatrix} = l \cdot M \cdot \begin{bmatrix} X - X_L \\ Y - Y_L \\ Z - Z_L \end{bmatrix} \tag{8}$$

in which vector $[x\ y\ -f]^T$ represent image space coordinates, l is a scale factor and vector $[X\ Y\ Z]^T$ represents the object point in world coordinates. The values of these two vectors are the outcome of the previously described georeferencing. The vector $[X_L\ Y_L\ Z_L]^T$ is the camera sensor position in world coordinates. The matrix M, like matrix P in equation (1), rotates the world coordinates into camera sensor coordinates and is in our case represented by the quaternion Q rather than a direct cosine matrix with euler angles. The new equation with the

quaternion transformation is shown in formula (9).

$$\begin{bmatrix} x \\ y \\ -f \end{bmatrix} = l \cdot Q \cdot q(v) \cdot \overline{Q} \tag{9}$$

The expression $q(v)$ is the quaternion representation of vector v:

$$q(v) = 0 + (X - X_L)i + (Y - Y_L)j + (Z - Z_L)k \tag{10}$$

$\overline{Q}$ is the complex conjugated Q, containing the rotation of the camera.
Because the position of the satellite is received from GPS, it is considered precise enough to remain unchanged and will be used as camera position vector $[X_L\ Y_L\ Z_L]^T$. This decision is further discussed in the limitations section. With keeping the position, the optimization is left with the four missing parameters of the rotation quaternion Q.

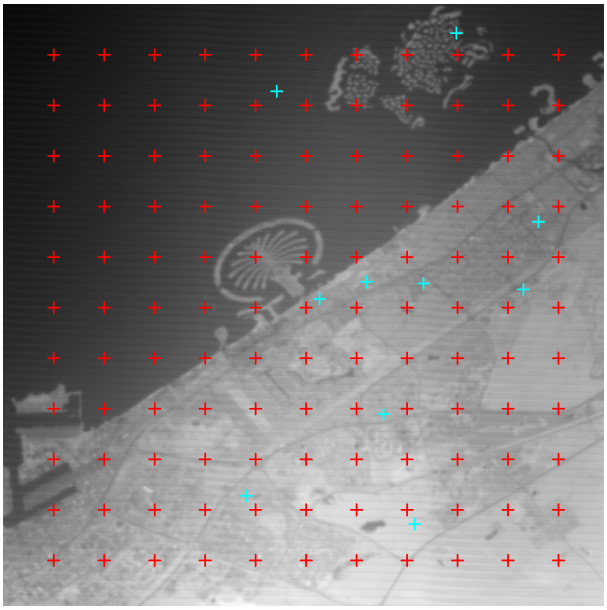

Figure 8: Regular grid (red) and random (cyan) image coordinates used for the minimization as $[x\ y]^T$

The minimization is done for 11x11 regular grid coordinates and 10 randomly distributed points for $[x\ y]^T$ with their corresponding world coordinates $[X\ Y\ Z]^T$. The image coordinates are shown in figure 8. With less points an oscillation in the yaw angle was observed.
A *Nelder-Mead*[5] minimization approach is used. Therefore equation (9) is reorganized into:

$$F_1 = x + f \cdot \frac{U}{W} \tag{11}$$

$$F_2 = y + f \cdot \frac{V}{W} \tag{12}$$

with

$$[U\ V\ W]^T = Q \cdot q(v) \cdot \overline{Q} \tag{13}$$

The factor l can be eliminated during this process.
The *Nelder-Mead* approach iteratively finds a solution by minimizing the squared sum:

$$R = F_1^2 + F_2^2 \tag{14}$$

As start values for the minimization, the attitude quaternion measured by the satellite is used.

Precision Validation

The outcome of the resection process is the true attitude quaternion for the satellite's near infrared camera. To validate the resulting attitude it was used to create orthophotos as described earlier. The resulting image is expected to show no deviation when overlayed to the sentinel image. However, visual inspection showed an offset of a few pixel at the borders of some images as shown in figure 9. This deviation might show image distortions and will be further investigated in the future.

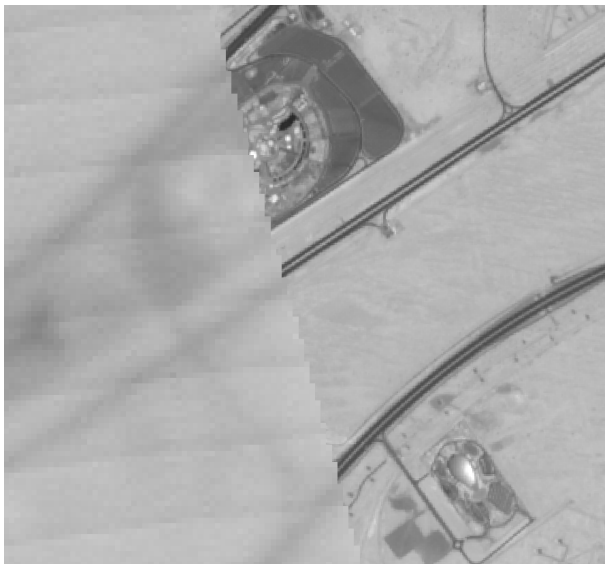

Figure 9: Zoomed view of the Sentinel image (right) with orthorectified MICS image overlayed (left) using the true attitude from the resection

The output quaternion of the minimization, representing the true satellite attitude for the MICS image, can now be compared to the attitude measured by the satellite.

ATTITUDE CORRECTION

Flying Laptop uses the common body coordinate system which aims the z-axis to the target and the x-axis perpendicular to the orbit normal. The orbit normal is defined as the cross product of the position and velocity vector. The y-axis completes the target system. Therefore, the rotation around the z-axis corresponds to the yaw. Following that the x-axis rotation is the roll and around the y-axis is the pitch.

The difference between this target attitude and the true attitude of the camera sensor is mainly determined by two factors. The first one is the static portion as a result from the slightly tilted installation of the cameras. The uncertainty of this part is believed to be in the order of $0.5\,\mathrm{deg}$ in relation to the star cameras, caused by mounting tolerances. As a second deviation, the dynamic satellite's attitude control system behavior comes to mind.
The static part was estimated by an inertial-orientated pointing, which allows the usage of the MICS as star cameras. This results in a very stable system because of low rotation rates. However, the MICS needs a fairly long integration time of multiple seconds to have visible stars in the photo. Therefore, dynamic effects will cause a visible blur of the stars. Hence, the static error can only be reduced to the level of the dynamic error. However, this error is expected to be lower in the inertial pointing than in a target overflight. Due to the method used to determine the attitude from star pictures, the yaw error was not corrected. This initial guess was then used as $R_{MountingBias}$ in equation (4).
Although, the dynamic part is smaller, it is the far more problematic, since it can not been calibrated out. In addition, its distribution is unknown because it has various origins. It mainly consists of the unknown noise on the star camera solutions and aliasing issues due to low sampling frequency of the rotation rate. Also, the controller error is part of this dynamics as well. The last part is a systematic error that is caused by a dependency of the pointing accuracy to another parameter like the target's latitude or longitude.
Taking the result of the resection as better estimate of the true attitude, the pointing error can be calculated. With the assumption that the dynamic part of the deviations is equally distributed over a large amount of pictures, the static part can be found. After removing the static part, the dynamic noise will be investigated. This investigation includes correlations with various satellite parameters. These parameters can entail the latitude of the target, elevation of the passage or satellite sensor metadata. Also, as the process is intended to run automatically, it will be used to monitor the overall pointing performance continuously.

LIMITATIONS

A major influence to the outcome of the proposed image processing is the successful image alignment of the MICS images with the sentinel data. The difficulty is a result of the varying image quality of the raw *Flying Laptop* satellite images due to several factors including cloud coverage, lightning conditions, earth surface properties and camera settings. A significant improvement of the stability of the georeferencing part of the alignment is expected with a better prealignment. This will be achieved with a better pointing knowledge of the satellite as an outcome of the approach described in this paper.

Another influence to the outcome of the image processing is the possible ambiguity of the results. There might be different attitude and position combinations that can result in the same picture. This effect is worse if the satellite position is also optimized as part of the resection. The influence can be divided in two parts. As one part of this problem, distortions, still existing in the images are identified. These distortions can have their origin in the camera optics or atmospheric effects. Another part is the limited MICS resolution. The resolution of $25\,\mathrm{m}$ per pixel results in a field of view of roughly $7.3''$ per pixel. This limits the precision of the resection as the image would show the same scene with the camera being rotated by this angle. It has to be defined in future effort, how this limitation can be circumvented, for example matching raw MICS images with data of a higher resolution.

In addition, to the limitations of the process itself, the meta data from the satellite used in the optimization has some accuracy limitations. There is an unknown delay between the command of the OBC and the real trigger of the picture. It is estimated to be within the order of $200\,\mathrm{ms}$. As the position information is recorded at the moment the OBC commands the PLOC, this information is outdated as well. The exact time of the picture is taken from the internal clock of the PLOC. The internal time of the PLOC is updated from the OBC every five minutes. In the worst case, this time update has the same delay as the picture command. Therefore, the knowledge of the position or time is limited by the time delay between the OBC and the PLOC.

Another issue is the satellite's velocity. The expected target system of *Flying Laptop* aims the x-axis perpendicular to the orbit normal. As the error in the time and position is unknown, the velocity vector is taken from the closest telemetry packet. In the case shown in the result section this packet has an interval of $1\,\mathrm{s}$. With a maximum delay of $200\,\mathrm{ms}$, this results in a worst case deviation of $700\,\mathrm{ms}$. Therefore, the maximum error is estimated to be $180''$. This causes an error in the yaw-axis.

RESULTS

The result of the resection is a new attitude information at the specific position and time. This attitude is compared with the target attitude of the satellite at this time. At this point this is executed only for a part of all images. The results shown beneath are based on a Dubai pointing from the 29th of May 2019. The comparison of the pitch and roll error angles are shown in figure 10. The pitch and roll error is in the desired order, although the pitch is slightly too high in the end.

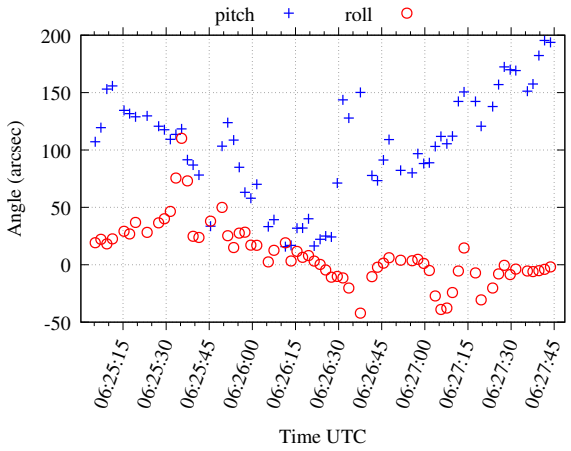

Figure 10: Roll and pitch error

The point of maximum elevation over the target is reached at 06:26:23 UTC. In contrast to our expectations, the error is decreasing towards the point but significantly increasing in pitch right afterwards. Overall the pitch error is positive during the whole pass. This might be caused by a static offset of $108.8''$. The standard deviation σ of the pitch angle is $47.0''$ and $26.4''$ for the roll axis.

The yaw error is larger but seems to have a static offset as well, as shown in figure 11. The median of the error is $687.4''$ with $\sigma = 141.76''$. Therefore, there seems to be inaccuracy with the yaw axis during the overflight.

Two pictures seem to have an invalid result for the yaw angle. The reason for this is currently unknown, as pitch and roll errors of the same pictures do not show a data jump. However, the yaw error is expected to be slightly larger, due to limitations mentioned before.

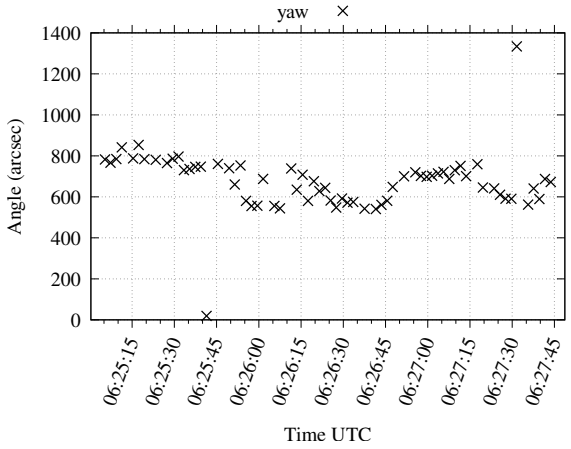

Figure 11: Yaw error

With the new static offset, new pointings will be commanded and the resection procedure will be reapplied to the results. As only a few target pointing are processed so far, there is no further investigation on the dynamic attitude noise. This will be executed when the resection is fully automated.

CONCLUSION

With an orthorectification, using only satellite information, an estimation of the captured scene can be made. This is a sufficient input for an algorithm aligning selected satellite images with already georeferenced scenes. Based on the results of aligning these images, the presented image processing procedure is able to determine a better fit for the true satellite's attitude. This can be verified by mapping images with the newly calculated attitude on the surface of the earth.

The resulting difference between the attitude measured by the satellite and the newly calculated one is in the expected range. Further calibration based on the results allows to correct the static part caused by the misalignment of the camera.

With the ability to process more images, the dynamic effects will be further observed. This will deliver a more precise knowledge of the target pointing for the optical data downlink.

Acknowledgments

The launch and operations of the *Flying Laptop* satellite has been funded by the Federal Ministry for Economic Affairs and Energy of Germany (BMWi) and by the ministry of economy, science and art of Baden-Württemberg. The used height model data was obtained from the ALOS mission results of the Japan Aerospace Exploration Agency. The ESA Copernicus hub and specifically Sentinel 2 images were used as reference data.

References

[1] Fuchs, C., Moll, F., Giggenbach, D., Schmidt, C., Keim, J., and Gaißer, S., "OSIRISv1 on Flying Laptop: Measurement Results and Outlook," 11 2019.

[2] Hartley, R. and Zisserman, A., *Multiple View Geometry in Computer Vision*, Cambridge books online, Cambridge University Press, 2003.

[3] Evangelidis, G. D. and Psarakis, E. Z., "Parametric Image Alignment Using Enhanced Correlation Coefficient Maximization," *IEEE Transactions on Pattern Analysis and Machine Intelligence*, Vol. 30, No. 10, 2008, pp. 1858–1865.

[4] Mikhail, E., Bethel, J., and McGlone, J., *Introduction to modern photogrammetry*, No. Bd. 1, Wiley, 2001.

[5] Nelder, J. A. and Mead, R., "A Simplex Method for Function Minimization," *The Computer Journal*, Vol. 7, No. 4, 01 1965, pp. 308–313.